The 2009 IEEE/RSJ International Conference on
Intelligent Robots and Systems
October 11-15, 2009 St. Louis, USA

Design and Implementation of a 12-Axis Accelerometer Suite

Chi-Wei Ho and Pei-Chun Lin

Abstract— We report on a 12-axis accelerometer suite which utilizes 12-axis linear acceleration measurements from four 3-axis accelerometers. This system is capable of deriving linear acceleration, angular acceleration and angular velocity via simple matrix operations. It also releases the requirement of accelerometer installation at the center of mass as well as eliminates the necessity of gyro implementation as in the traditional inertia measurement unit (IMU). An optimal configuration of the system is proposed based on the analysis of rigid body dynamics and matrix theory. We also report the results of experimental evaluation. We believe the analysis presented in this paper would benefit the practical design of IMUs in the future.

I. INTRODUCTION

For several decades, inertial sensors [1] have been one of the important categories of sensors utilized in various applications, including navigation (robots, vehicles, rockets, and etc) [2]–[5], state estimation for motion analysis [6] or dynamic modeling, microsurgery [7], [8], and sports injury avoiding [9], [10]. In modeling dynamics of legged robots, information of external forces, position and orientation states (including their 1st/2nd derivatives) are usually required as essential information for constructing 2nd-order dynamic models, and the inertial sensors are the appropriate choices to provide some essential information of states. A traditional inertial measurement unit (IMU) is comprised of 3-axis acceleration measurement by accelerometers installed at the center of mass (COM) and 3-axis angular velocity measurement by rate gyros. Though full position/orientation states can be reconstructed by models and filter technologies such as the Kalman filter [11], such systems usually yield poor performance and generate unbounded integration error due to their nature of unobservability [12]. Thus, techniques of fusing IMU with other positioning sensors (GPS [13], differential GPS, magnetocompass, and vision system [14]) are widely adapted.

While translational displacement, velocity, and acceleration as well as orientation and angular velocity can all be measured by commercially available sensors, the only state left unknown is angular acceleration. To solve this, accelerometer-based systems are widely investigated because accelerometers are low-cost and easily calibrated by gravity, and more importantly, the linear acceleration measured by accelerometer is related to the angular acceleration and the angular velocity in a specific mathematical equation (total 9 scalar unknowns) based on Newton Mechanics (detailed in (1)). Thus, for decades researchers have tested various methods attempting to recover all three states (totally 9 scalar unknowns) via a minimum set of sensors together with specific computational algorithms. A system with 6 scalar measurements can theoretically solve all nine unknowns, but in reality integration error involved in the computation quickly deteriorates the accuracy. King et. al. [17], [18] proposed a 9-axis acceleration measurement system capable of deriving bounded linear and angular acceleration, but no information on angular velocity. Chen et. al. [19] proposed a novel 6-axis system with bounded angular acceleration, but linear acceleration became unbounded. Park et. al. [20] improved the previous system with three extra axes of measurements. Using the same cube-shape geometric configuration of sensors as [19], [20], later Parsa et. al. [21] proposed a system comprised of twelve 1-axis accelerometers to yield all states. In recent years with the advanced development in micro electro-mechanical-systems (MEMS), multi-axis MEMS accelerometers have become commercially available, low-cost yet with promising performance. In addition, it also grants the orthogonality among all three measuring axes. All these reasons motivate authors to revisit the question of how to select, place, and orient accelerometers, especially with multi-axis ones, to yield better performance and feasible solutions for practical implementation.

Here, we investigate a 12-axis accelerometer suite containing 12-axis linear acceleration measurements from four 3-axis accelerometers at four distinct locations. Comparing to the traditional IMU, this suite has following advantages: (1) it provides instant angular acceleration and angular velocity derivation via linear operation without any differentiation or integration; (2) the positioning of four 3-axis accelerometers is flexible, which releases the strong constraint of accelerometer installation at COM in the traditional IMU; (3) it does not require gyros; thus avoiding implementation of a second type of sensors and its complicate calibration procedure. Moreover, since all accelerometers are 3-axis and mutually orthogonal to each other, the sensor orientation error due to installation can be thoroughly eliminated through a calibration procedure which defines a rotational matrix relating the principal axes of the body and the measuring directions of the sensor.

Section II introduces the idea of this 12-axis accelerometer-based system based on the analysis of rigid

This work is supported by National Science Council (NSC), Taiwan, under contract NSC 97-2218-E-002-022 and by Tzong Jwo Jang Educational Foundation under contract 97-S-A07.

Authors are with Department of Mechanical Engineering, National Taiwan University, No.1 Roosevelt Rd. Sec.4, Taipei, Taiwan, Corresponding email: peichunlin@ntu.edu.tw

body dynamics, followed by Section III which describes the positioning of sensors in detail. Section IV reports the technique of deriving angular velocity, and Section V briefly describes the calibration procedure. Section VI reports the results of experimental evaluation, and Section VII concludes the work.

II. CONSTRUCTION OF THE SENSING SYSTEM

The acceleration vector, $\mathbf{a}_p$, in an inertial frame $\mathcal{W}$ of a point, p, rigidly attached to an accelerating body frame $\mathcal{B}$ with origin, o, is a function of the body's angular velocity, ω, and angular acceleration, $\dot{\omega}$, as well as the translational acceleration of the body origin, $\mathbf{a}_o$, given by

$$\mathbf{a}_p = \mathbf{a}_o + \dot{\omega} \times \mathbf{r}_{op} + \omega \times (\omega \times \mathbf{r}_{op}), \tag{1}$$

where $\mathbf{r}_{op}$, the fixed position vector of p relative to the body, is presumed known á priori. In general, we are interested in the motion of the body relative to the world. Hence, we seek to extract from measurements of the left-hand quantities to derive right-side unknown body states, including the COM translational acceleration, $\mathbf{a}_{COM}$, (usually equal to the origin of body frame, $\mathbf{a}_o$), angular acceleration, $\dot{\omega}$, and angular velocity, ω,

$$\begin{array}{rcl} \mathbf{a}_o & = & \mathbf{a}_{COM} = \left[\begin{array}{ccc} a_x & a_y & a_z \end{array}\right]^T \\ \dot{\omega} & = & \left[\begin{array}{ccc} \dot{\omega}_x & \dot{\omega}_y & \dot{\omega}_z \end{array}\right]^T \\ \omega & = & \left[\begin{array}{ccc} \omega_x & \omega_y & \omega_z \end{array}\right]^T. \end{array}$$

Note that the angular velocity in (1) appears in a quadratic form; hence, by defining a function

$$\mathbf{q}(\omega) = \left[\begin{array}{cc} \omega_i^2 + \omega_j^2 & \omega_i\omega_j \end{array}\right]^T \quad i < j \in 1,2,3 \tag{2}$$

where the six distinct second-degree monomials of $\omega \times \omega$ formed from the three unknowns of ω, (1) is now linear to 12 unknowns, $\mathbf{x}_{var}$:

$$\mathbf{x}_{var} = \left[\begin{array}{ccc} \mathbf{a}_{COM}^T & \dot{\omega}^T & \mathbf{q}(\omega)^T \end{array}\right]^T, \tag{3}$$

thereby establishing that the determination of the original nine unknowns in (2) reduces to a linear computation that we will proceed to detail, at the expense of requiring three additional measurements beyond the nine intrinsic dimensions of the data.

The 1-axis accelerometer installed at the point, p, on the body measures the projected linear acceleration of spatial body motion, ${}^b\mathbf{a}_p$, along the sensing direction $\hat{\mathbf{s}_j}$,

$${}^b a_j = \mathbf{a}_p \cdot \hat{\mathbf{s}_j} = [\mathbf{a}_o + \dot{\omega} \times \mathbf{r}_{op} + \omega \times (\omega \times \mathbf{r}_{op})] \cdot \hat{\mathbf{s}_j}, \tag{4}$$

where the motion is with respect to the inertial frame but the coordinates are represented in the body frame (i.e. letter "b" on the upper left corner of the state). Since the position vector, $\mathbf{r}_{op}$, and sensing direction, $\hat{\mathbf{s}_j}$, are invariant with respect to the body frame $\mathcal{B}$, it motivates us to represent the coordinate of dynamic equation (1) at every instant in the body frame while the measured states of the moving body are still with respect to the inertial frame:

$${}^b\mathbf{a}_p = {}^b\,\mathbf{a}_o + {}^b\,\dot{\omega} \times {}^b\,\mathbf{r}_{op} + {}^b\,\omega \times ({}^b\omega \times {}^b\,\mathbf{r}_{op}). \tag{5}$$

In the following text all the equations will be represented in the body coordinates, and the notations "b" on the upper left corners will be omitted for clear equation presentations.

Presumably we have twelve 1-axis linear acceleration measurements from the accelerometers, $\mathbf{a_m}$,

$$\mathbf{a_m} = \left[\begin{array}{cccc} a_1 & a_2 & \ldots & a_{12} \end{array}\right]^T$$

with known sensor positions, $\mathbf{r_m}$, and orientations, $\hat{\mathbf{s}}$, on the body

$$\begin{array}{rcl} \mathbf{r_m} & = & \left[\begin{array}{cccc} \mathbf{r}_1^T & \mathbf{r}_2^T & \ldots & \mathbf{r}_{12}^T \end{array}\right]^T \\ \hat{\mathbf{s}} & = & \left[\begin{array}{cccc} \hat{\mathbf{s}_1}^T & \hat{\mathbf{s}_2}^T & \ldots & \hat{\mathbf{s}_{12}}^T \end{array}\right]^T. \end{array}$$

Without loss of generality, the sensing directions of accelerometers, $\hat{\mathbf{s}_k}_{\ k=1,\ldots,12}$, can be set to align with three principal axes of the body frame, $\hat{\mathbf{s}_k}_{\ k=1,4,7,10} = \hat{\mathbf{e}_x}, \hat{\mathbf{s}_k}_{\ k=2,5,8,11} = \hat{\mathbf{e}_y}, \hat{\mathbf{s}_k}_{\ k=3,6,9,12} = \hat{\mathbf{e}_z}$. Thereby, twelve 1-axis accelerometers measure the linear accelerations of the body along the three principal axes directly, each with four measurements for symmetrical consideration. Instead of computing the inner product described in (4), computation in the current arrangement of sensing directions only requires the selection of one out of three scalar components of the dynamic equation (5). Thus, the left side of (5) can directly be represented by $\mathbf{a_m}$, and the system comprised by the above 12 scalar equations can be represented as

$$\mathbf{a_m} = \mathbf{S}(\mathbf{r_m})\mathbf{x}_{var}. \tag{6}$$

The 12 unknown scalar states, $\mathbf{x}_{var}$, on the right-side of the equation can thereby be linear computed by the following matrix operation:

$$\mathbf{x}_{var} = \mathbf{S}(\mathbf{r_m})^{-1}\mathbf{a_m}. \tag{7}$$

Since $\mathbf{r_m}$ is known a priori, the extraction of the desired state, $\mathbf{x}_{var}$, now hinges upon the rank and numerical condition of the 12×12 "structure" matrix $\mathbf{S}(\mathbf{r_m})$, which is solely a function of the positions of the accelerometers, $\mathbf{r_m}$.

III. SENSOR ALLOCATION

The rise of MEMS sensing technology has yielded commercially available low-cost MEMS accelerometers that have better performance, lower prices, and smaller packaging than those of a decade ago. More importantly, the availability of multi-axis MEMS accelerometers[1]

[1]For example, Analog Devices Inc, Freescale Semiconductor, VTI Technologies, Measurement Specialties Inc/Schaevitz, and STMicroelectronics all produce 3-axis MEMS-based accelerometers.

significantly simplifies the original complicated electronic design and spatial layout of multi-sensor systems for multi-axis state measurements. Therefore, in the following work we utilize four 3-axis accelerometers shown in Figure 1 in the design of the 12-axis acceleration measurement system described in the previous Section II, and focus on how to appropriately allocate these four accelerometers spatially so the system is capable of yielding trustable numerical operations defined in (7).

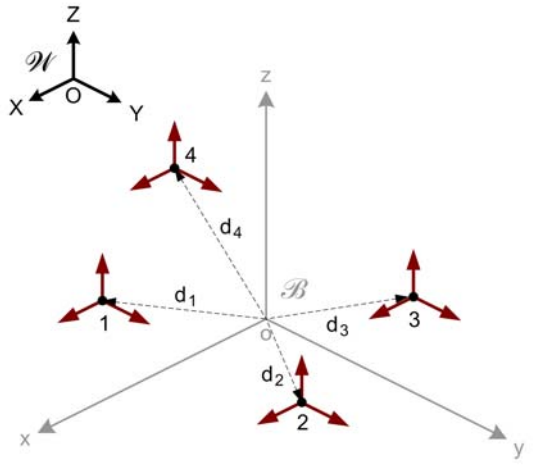

Fig. 1. 12-axis accelerometer suite: four 3-axis accelerometers are located at four distinct positions on the body, and each accelerometer measures linear accelerations in the directions parallel to the three principal axes of the body frame.

In the IMU system comprised by four 3-axis accelerometer, the twelve 1-axis scalar acceleration measurement, $\mathbf{a_m}$, is represented by four 3-axis acceleration measurements

$$\begin{aligned} \mathbf{a_m} &= \begin{bmatrix} \mathbf{a}_1^T & \mathbf{a}_2^T & \mathbf{a}_3^T & \mathbf{a}_4^T \end{bmatrix}^T \\ \mathbf{a}_k &= \begin{bmatrix} a_{kx} & a_{ky} & a_{kz} \end{bmatrix}_{k=1,2,3,4}, \end{aligned}$$

and $\mathbf{r_m}$ is comprised of four distinct spatial positions of accelerometers

$$\begin{aligned} \mathbf{r_m} &= \begin{bmatrix} \mathbf{r}_1^T & \mathbf{r}_2^T & \mathbf{r}_3^T & \mathbf{r}_4^T \end{bmatrix}^T \\ \mathbf{r}_k &= \begin{bmatrix} r_{kx} & r_{ky} & r_{kz} \end{bmatrix}_{k=1,2,3,4}. \end{aligned} \tag{8}$$

In this scenario, the system of equations shown in (6) is composed by four copies of dynamic equations shown in (5), and the structure matrix, $\mathbf{S}(\mathbf{r_m})$, can further be represented as

$$\mathbf{S}(\mathbf{r_m}) = \begin{bmatrix} 1 & 0 & 0 & 0 & -r_{1z} & r_{1y} & 0 & 0 & -r_{1x} & r_{1y} & r_{1z} & 0 \\ 0 & 1 & 0 & r_{1z} & 0 & -r_{1x} & 0 & -r_{1y} & 0 & r_{1x} & 0 & r_{1z} \\ 0 & 0 & 1 & -r_{1y} & r_{1x} & 0 & r_{1z} & 0 & 0 & 0 & r_{1x} & r_{1y} \\ 1 & 0 & 0 & 0 & -r_{2z} & r_{2y} & 0 & 0 & -r_{2x} & r_{2y} & r_{2z} & 0 \\ 0 & 1 & 0 & r_{2z} & 0 & -r_{2x} & 0 & -r_{2y} & 0 & r_{2x} & 0 & r_{2z} \\ 0 & 0 & 1 & -r_{2y} & r_{2x} & 0 & r_{2z} & 0 & 0 & 0 & r_{2x} & r_{2y} \\ 1 & 0 & 0 & 0 & -r_{3z} & r_{3y} & 0 & 0 & -r_{3x} & r_{3y} & r_{3z} & 0 \\ 0 & 1 & 0 & r_{3z} & 0 & -r_{3x} & 0 & -r_{3y} & 0 & r_{3x} & 0 & r_{3z} \\ 0 & 0 & 1 & -r_{3y} & r_{3x} & 0 & r_{3z} & 0 & 0 & 0 & r_{3x} & r_{3y} \\ 1 & 0 & 0 & 0 & -r_{4z} & r_{4y} & 0 & 0 & -r_{4x} & r_{4y} & r_{4z} & 0 \\ 0 & 1 & 0 & r_{4z} & 0 & -r_{4x} & 0 & -r_{4y} & 0 & r_{4x} & 0 & r_{4z} \\ 0 & 0 & 1 & -r_{4y} & r_{4x} & 0 & r_{4z} & 0 & 0 & 0 & r_{4x} & r_{4y} \end{bmatrix}.$$

We observe that the determinant of this structure matrix $\mathbf{S}(\mathbf{r_m})$ with 12 scalar position variables, $det(\mathbf{S}(\mathbf{r_m})$, is given by the determinant of the "sensor simplex" array, $det(R)$,

$$det(\mathbf{S}(\mathbf{r_m})) = (2det(\mathbf{R}))^3,$$

where $\mathbf{R} = \begin{bmatrix} \mathbf{r}_2 - \mathbf{r}_1 & \mathbf{r}_3 - \mathbf{r}_1 & \mathbf{r}_4 - \mathbf{r}_1 \end{bmatrix}$. Therefore, as long as the accelerometer suite shown in Figure 1 defines a spatial tetrahedron with nonzero volume (that is, the four 3-axis accelerometers are in a general position, such that there is no coplanar subset of any three of them), it provides, in principle, a complete "Advanced IMU": a means of extracting full 6-dimension rigid-body acceleration and 3-dimension angular velocity data, with no recourse to rate gyros at all.

Although the determinant of the structure matrix $\mathbf{S}(\mathbf{r_m})$ can be shown to reduce to that of the "simplex matrix", its condition number[2] determined by high-order polynomials (in the entries of the tetrahedron) is more complicated function of the shape of the tetrahedron the simplex matrix defines, yet there is every reason to validate that the condition number would be very sensitive to the "shape" and "size" of the tetrahedron and its location relative to COM. In practice, numerical exploration suggests that the optimal condition occurs when four 3-axis accelerometers are placed symmetrically coincident with the corners of a cube shown in Figure 2, which yields the best condition number $\sqrt{2}$.

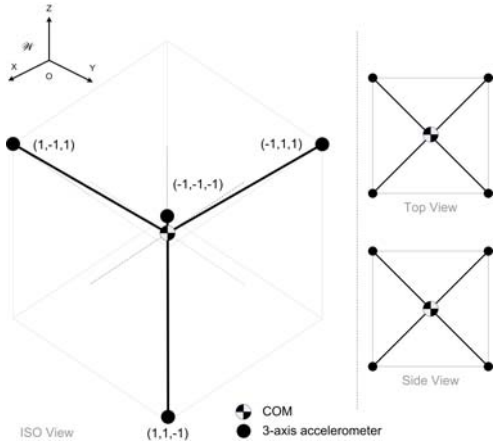

Fig. 2. The position allocation of the four 3-axis accelerometers which yields the best condition number of the structure matrix $\mathbf{S}(\mathbf{r_m})$.

Interestingly, the structure matrix combines entries with and without physical scale — for example, "1" in the first 3×3 identity matrix are dimensionless, but the second 3×3 skew-symmetric matrix has unit of "length", as well as the third and fourth 3×3 matrices. Thus, it turns out there is actually a preferred linear

[2]Defined as the ratio of the largest to the smallest singular values of the matrix, and singular values are equal to the square roots of eigenvalues of the symmetric square $\mathbf{S}^T\mathbf{S}$.

dimension of this cube at which the resulting condition number is optimal. For example, a physical installation of sensors with $l = 10cm$ should use "decimeter" as the unit which sets $l = 1$, not centimeter ($l = 10$), or meter ($l = 0.1$) which yield large condition number "$10\sqrt{2}$" and "10", respectively. The condition number of the matrix is purely determined by the relative magnitude of its matrix elements; thus, choose a right unit so that the magnitude of the elements close to the optimal condition will reduce the additional error induced by the matrix inversion.

Comparing to other arrangements of twelve 1-axis acceleration measurement system (i.e. twelve 1-axis, six 2-axis,etc), the usage of four 3-axis accelerometers requires less space and simpler electronic design. In addition, with the availability of acceleration measurements in all 3 axes at each sensor location, orientational installation error of sensors (i.e. measuring directions are not aligned with the principal axes) can be easily compensated by a simple rotational operator, which relates the orientational relation between directions of measurements of sensors and those of the principal axes of the body frame. This system with calibration significantly improves the accuracy of the measurements.

IV. DERIVATION OF THE ANGULAR VELOCITY

The process to obtain an invertible mapping for this quadratic system from $\omega \times \omega$ to ω can not be solved kinematically by the six available equations alone since there exists at least one sign ambiguity for the unknowns. In general, this kind of quadratic systems can be solved by the common numerical methods (ex: The Newton-Raphson Method, Secant Method, and etc). However, in our implementation on the embedded system with $1kHz$ sampling rate, the computation power of the microprocessor onboard is not high enough to finish the above numerical search of solutions in time.

Here we explore a simpler method which utilizes the initial conditions and the intrinsic integration-derivation relation between the angular velocity and the angular acceleration which is derived simultaneously in the same 12-axis accelerometer suite. Without loss of generality, assuming the angular acceleration and angular velocity are available at time t_i, the procedure to solve angular velocity at t_{i+1} is described as follows. First, combine both $\omega_i^2 + \omega_j^2$ and $\omega_i\omega_j$ derived in $\mathbf{x}_{var}$ to construct a set of complete-square equations, $(\omega_i + \omega_j)^2$ $_{i<j,i,j=1,2,3}$:

$$\begin{array}{rcl} \omega_1 + \omega_2 & = & \pm\sqrt{a} \\ \omega_1 + \omega_3 & = & \pm\sqrt{b} \\ \omega_2 + \omega_3 & = & \pm\sqrt{c}, \end{array} \tag{9}$$

where a, b, and c are values derived from the computed last six variables of $\mathbf{x}_{var}$ (i.e. $\mathbf{q}(\omega)$). Second, derive the "estimated" angular velocity at t_{i+1} from the values of the angular velocity at t_i and the angular acceleration at both t_i and t_{i+1},

$$\omega_{i+1} = \omega_i + \frac{1}{2}h(\dot{\omega}_i + \dot{\omega}_{i+1}), \tag{10}$$

where h denotes the sampling period [3]. (10) represents prediction of the angular velocity prediction via trapezium rule. Third, adopt the sign of "estimated" angular velocity derived in (10) as the correct sign to clear out the sign ambiguity shown in (9). Thus, the estimated angular velocity derived from integration is only used for sign check, and the magnitude of the angular velocity is still determined by the values derived from $\mathbf{q}(\omega)$ shown in (2).

V. CALIBRATION

If the sensing directions of the sensors do not align perfectly with their assigned directions (here, the principal axes), the sensors will respond to the accelerations in other axes, which cause severe state reconstruction errors, especially when the accelerations in different principal axes varying significantly with time. Assuming the 3-axis measurements in the MEMS accelerometers are mutually orthogonal to each other, the relation of these axes to the principal axes of the body frame is a rotation matrix. The parameters of the matrix can be found by performing a 3-dimensional rotation of the system: first, align the principal axes of the system to those of the world frame. Second, rotate the system slowly along with three principal axes of the world frame sequentially; in the meantime collect data of sensor measurements and actual body orientation in order to yield acceleration due to gravity. Then perform the least square technique to find the parameters.

VI. EXPERIMENT RESULTS

A benchtop apparatus with one controllable rotational degree of freedom shown in Figure 3(a) was utilized for experimental evaluation of the proposed system. The required measurements of four 3-axis accelerations of the IMU system were measured by four 3-axis accelerometers (ADXL330, Analog Device). In addition, a complete traditional IMU was also mounted for performance comparison (one ADXL330 accelerometer and three ADXRS610 gyros, Analog Device). A real-time embedded control system (sbRIO-9632, National Instruments) running at 1kHz was in charge of sinusoidal motion generation and sensor signal collection. All the body state ($\mathbf{a}_{COM}$, $\dot{\omega}$, and ω) were also computed and updated in the same embedded system at the same sampling rate. The 3-axis ADXL330 accelerometer chip itself (range 3g) have output noises $0.0742m/s^2$ in X and Y directions and $0.1039m/s^2$ in the Z direction, and the average measured root mean squared noises of the complete 3-axis accelerometer sensor module in X,Y and Z directions are about doubled — $0.1625m/s^2$

[3]Thus, the initial condition of the angular velocity is required. For example, $\omega_1 = \begin{bmatrix} 0 & 0 & 0 \end{bmatrix}$ if the computation starts when the body is static.

and $0.1803 m/s^2$, respectively. The noises of the linear accelerations derived from 12-axis system decrease to $0.0640 m/s^2$ and $0.0914 m/s^2$, comparable to the noises of the chip itself.

The COM of the IMU system was positioned on the rotating apparatus with designated distance, not at the rotation center of turntable as shown in Figure 3(b). Thus, the simulated COM was subjected to tangential, normal, and angular accelerations while the turntable rotated. A PD position control was utilized to drive the turntable in the sinusoidal motion, and the "desired" acceleration was derived from position sinusoidal curve directly. In the first set of measurement, direction of the rotating axis of the apparatus was parallel to the direction of gravity, so the acceleration induced by gravity did not affect the experimental measurements. In the second set of measurement the turntable was tilted while rotating, so in this scenario the motion acceleration and gravity induced acceleration are coupled. We utilized a 2-axis inclinometer (SCA100T-D02, VTI) which was capable of detecting the direction of the gravity. The gravity acceleration was compensated from measured acceleration before the data was imported into the proposed algorithm.

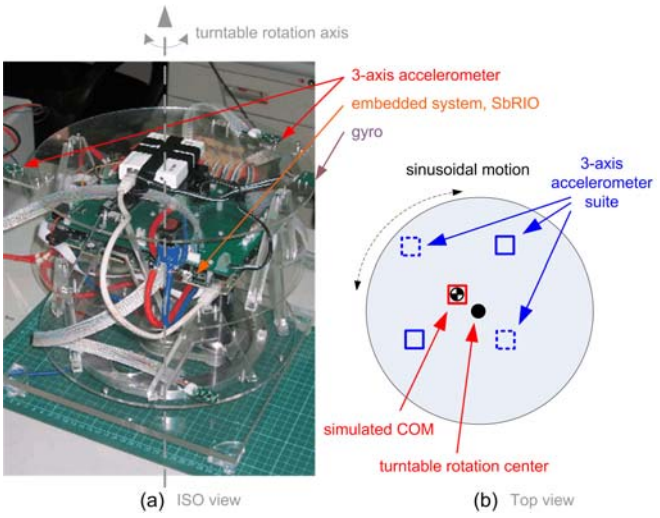

Fig. 3. The experiment apparatus: (a)picture (b)system arrangement

Figure 4 illustrates the body states of desired and experimental measurements, including data from the 12-axis accelerometer suite and the traditional IMU. Because of the unavoidable vibration of apparatus during reciprocal rotational motion as well as the simple PD position control, the experimentally measured states yield slightly measurement noises comparing to the desired curve, but all states display similar measurement from that of the traditional IMU. The 12-axis accelerometer suite delivers reliable measurement of the linear acceleration at COM compared with that from the traditional IMU which directly measures the state at the COM.

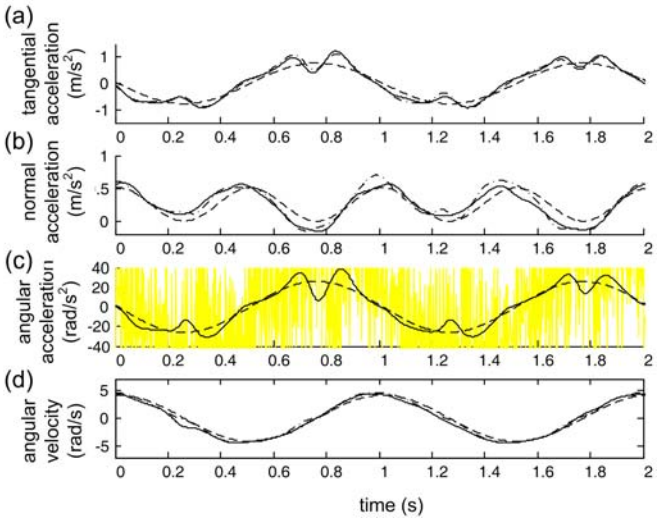

Fig. 4. Plots of the desired (dashed lines) and the experimental measured body states (solid lines: the 12-axis accelerometer suite; dotted lines: the traditional IMU).

Figure 4(a) and (b) indicate that one of the merits of the 12-axis accelerometer suite can indeed be achieved — releasing the necessity of direct linear acceleration measurement at the COM as in the traditional IMU, and the root mean squared errors (RMSE) between these two are $0.0609 m/s^2$ (tangential) and $0.0567 m/s^2$ (normal), respectively. While the traditional IMU derives noisy angular acceleration via differentiation of the angular velocity measurement from the rate gyros, the 12-axis accelerometer suite validates the second merit — the angular acceleration can be derived by simple linear computation shown in Figure 4(c). The comparison of these two to the desired curve are $6.5789 rad/s^2$ (12-axis system) and $64.71 rad/s^2$ (traditional IMU), respectively. In addition, Figure 4(d) indicates that the 12-axis accelerometer suite delivers comparable angular velocity measurement in comparison with that from the rate gyro (RMSE: $0.167 rad/s$). This confirms the third merit of the 12-axis IMU — obtaining accurate angular velocity without the rate gyro installation.

Figure 5 shows the acceleration of COM in the sinusoidal rotation test while the turntable was tilted. Gravity induced sinusoidal acceleration was clearly observed in the uncompensated curves. Accelerations in the compensated system performed much better in tracking the desired curve, but not as good as the previous test due to extra errors resulted from the inclinometer. We are currently investigate suitable orientation sensors with higher bandwidth for better performance of gravity compensation.

VII. CONCLUSIONS AND FUTURE WORKS

We have investigated a 12-axis accelerometer suite which utilizes acceleration measurements from four 3-axis accelerometers. Construction of this IMU system

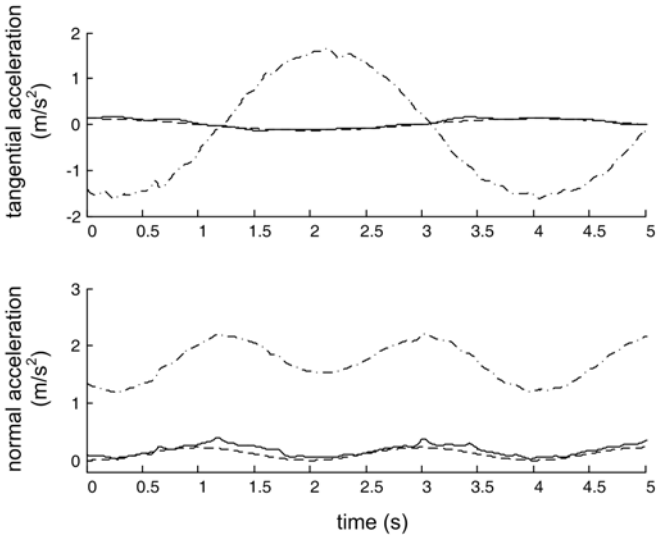

Fig. 5. Plots of the theoretical (dash lines) and the experimental measured body states (solid lines: gravity compensated; dash-dotted lines: uncompensated).

was based on the analysis of rigid body dynamics and matrix theory, and an optimal configuration of the system was proposed. We have reported a simple and efficient technique of deriving the angular velocity from its quadratic formulation in the dynamic equation. The experimental results confirmed several benefits of this 12-axis accelerometer suite. First, though the accelerometers are not installed at the COM, it is still capable of delivering measurement of the linear acceleration at the COM with comparable accuracy in comparison with that measured by the traditional IMU. Second, it yields correct measurement of the angular acceleration via simple matrix operation without any differentiation or integration process. Third, it is capable of deriving bounded angular velocity, without any consolation of gyros; thus avoiding the possible saturation problem and complicated calibration procedure of the gyros.

Currently we are in the process of testing the system in reality under various different accelerating conditions. In the meantime, we are searching for suitable position and orientation sensors to be fused with the proposed suite, thus to better compensate the gravity effect and to construct an observable system capable of delivering accurate full body state estimation for analysis of dynamic locomotion in the legged robots.

VIII. ACKNOWLEDGMENTS

This work is supported by National Science Council (NSC), Taiwan, under contract NSC 97-2218-E-002-022 and by Tzong Jwo Jang Educational Foundation under contract 97-S-A07.

References

[1] N. Barbour and G. Schmidt, "Inertial sensor technology trends," IEEE Sensors Journal, vol. 1, no. 4, pp. 332–339, 2001.

[2] R. L. Greenspan, "Inervial navigation technology from 1970-1995," Jounral of the Institute of Navigation, vol. 42, no. 1, pp. 165–185, 1995.

[3] B. Barshan and H. F. Durrant-Whyte, "Inertial navigation systems for mobile robots," IEEE Transactions on Robotics and Automation, vol. 11, no. 3, pp. 328–342, 1995.

[4] J. L. Weston and D. H. Titterton, "Modern inertial navigation technology and its application," IEEE Electronics and Communication Engineering Journal, vol. 12, no. 3, pp. 49–64, 2000.

[5] C.-W. Tan and S. Park, "Design of accelerometer-based inertial navigation systems," IEEE Transactions on Instrumentation and Measurement, vol. 54, no. 6, pp. 2520–2530, 2005.

[6] D. Giansanti, V. Macellari, G. Maccioni, and A. Cappozzo, "Is it feasible to reconstruct body segment 3-d position and orientation using accelerometric data?" IEEE Transactions on Biomedical Engineering, vol. 50, no. 4, pp. 476–483, 2003.

[7] W. T. Ang, P. K. Khosla, and C. N. Riviere, "Design of all-accelerometer inertial measurement unit for tremor sensing in hand-held microsurgical instrument," in IEEE International Conference on Robotics and Automation, 2003, pp. 1781–1786.

[8] ——, "Nonlinear regression model of a low-g mems accelerometer," IEEE Sensors Journal, vol. 7, no. 1, pp. 81–88, 2007.

[9] J. J. Crisco, J. J. Chu, and R. M. Greenwald, "An algorithm for estimating acceleration magnitude and impact location using multiple nonorthogonal single-axis accelerometers," Journal of Biomechanical Engineering, vol. 126, no. 6, pp. 849–854, 2004.

[10] P. Cappa, L. Masia, , and F. Patane, "Numerical validation of linear accelerometer systems for the measurement of head kinematics," Journal of Biomechanical Engineering, vol. 127, no. 6, pp. 919–928, 2005.

[11] R. E. Kalman, "A new approach to linear filtering and prediction problems," Transactions of the ASME – Journal of Basic Engineering, vol. 82, no. Series D, pp. 35–45, 1960.

[12] P. Lin and H. Komsuoglu and D. E. Koditschek, "Sensor data fusion for body state estimation in a hexapod robot with dynamical gaits," IEEE Transactions on Robotics, vol. 22, no. 5, pp. 932–943, 2006.

[13] D. T. Knight, "Rapid development of tightly-coupled gps/ins systems," IEEE AES Systems Magazine, vol. 12, no. 2, pp. 14–18, Feb 1997.

[14] S. I. Roumeliotis, A. E. Johnson, and J. F. Montgomery, "Augmenting inertial navigation with image-based motion estimation," in IEEE International Conference on Robotics and Automation, 2002.

[15] A. J. Padgaonkar, K. W. Krieger, and A. I. King, "Measurement of angular accelerarion of a rigid body using linear accelerometers," Transactions of the ASME, vol. 42, pp. 552–556, 1975.

[16] N. K. Mital and A. I. King, "Computation of rigid-body rotation in three-dimensional space from body-fixed linear acceleraion measurments," Journal of Applied Mechanics, vol. 46, pp. 925–930, 1979.

[17] J. Chen, S. Lee, and D. B. DeBra, "Gyroscope free strapdown inertial measurement unit by six linear accelerometers," Journal of Guidance, Control, and Dynamics, vol. 17, no. 2, pp. 286–290, 1994.

[18] S. Park, C.-W. Tan, and J. Park, "A scheme for improving the performance of a gyroscope-free inertial measurement unit," Sensors and Actuators A, vol. 121, no. 2, pp. 410–420, 2005.

[19] K. Parsa, T. A. Lasky, and B. Ravani, "Design and implementation of a mechatronic, all-accelerometer inertial measurement unit," IEEE/ASME Transactions on Mechatronics, vol. 12, no. 6, pp. 640–650, 2007.